ARTICLE

Multifunctional Hydrophobin: Toward Functional Coatings for Drug Nanoparticles

Hanna K. Valo,[†,*] Päivi H. Laaksonen,[‡] Leena J. Peltonen,[†] Markus B. Linder,[‡] Jouni T. Hirvonen,[†] and Timo J. Laaksonen[†]

[†]Division of Pharmaceutical Technology, P.O. Box 56, FI-00014, University of Helsinki, Finland, and [‡]VTT Biotechnology, VTT Technical Research Center of Finland, Tietotie 2, Espoo, P.O. Box 1000, FI-02044 VTT, Finland

ABSTRACT Efficient delivery of nanosized drug formulations to the desired body sites is not always reached despite the rapid development of pharmaceutical nanotechnologies. In spite of the undoubted effect of the size for increased bioavailability and controlled drug delivery, submicrometer formulations also require a deeper level of design. The surface properties of the particles determine the stability of the particles, interactions with the body, and targeting potentials of drugs. Thus, the efficacy of the drug can be increased utilizing the surface layer of the nanoparticles. Influencing the surface characters of the drug is the main focus of the present work, which introduces a method for preparing nanoparticles with functional sites from low-solubility drugs using hydrophobin (HFB) proteins. Particles were prepared by precipitating a lipophilic drug (beclomethasone dipropionate) in water in the presence of the HFB proteins. Particle size below 200 nm could easily be reached with increasing HFB concentration. The particles were shown to be stable for at least 5 h in suspension, and they could be stored for longer periods of time after freeze-drying. Labeling studies using green fluorescent protein (GFP) genetically fused to a HFB clearly demonstrated that the surface of the nanoparticles was covered with the hydrophobins and that the surface could be further modified by utilizing fusion proteins. This provides a template for a variety of different functional surface-bound groups that could be tailored by modifying the hydrophilic side of the HFB *via* protein bioengineering. In this study, the combination of proteins and traditional pharmaceutical technology was used to synthesize functionalized protein-coated nanoparticles for drug delivery purposes.

KEYWORDS: nanoparticles · hydrophobins · fusion proteins · beclomethasone dipropionate · labeling · functionalization

Nanotechnology has provided many improvements in the processing and formulation of materials. In many cases, nanoscopic size is beneficial for instance in providing better matrix dispersion in composite materials, in enhancing controlled release of molecules, or in increasing solubility. Here we show how an advanced bottom-up approach in drug formulation can be used as a tool to overcome some of the key problems in drug delivery. The major problems in delivering solid drugs include poor aqueous solubility of the pharmaceutically active ingredients, poor permeation properties, and stability problems in the gastrointestinal (GI) tract, due to which many highly potent drugs fail to reach commercialization. Nanoparticles as drug carriers offer several possibilities to improve the bioavailability of these problematic drug compounds. In addition to the small size, by modifying other physicochemical properties of the drug carrier system more efficient drug targeting strategies can be achieved.[1−3]

Several methods and materials are available to synthesize small, monodisperse particles of different shapes and surface coatings. Precipitation is a commonly used, well-known bottom-up method to produce nanosized particles.[4−7] In the antisolvent precipitation method very small particles are formed because of sudden supersaturation when a dissolved material is mixed with an antisolvent. The solvent, solvent/antisolvent ratio, stirring rate, temperature, and selection and amount of stabilizer are the critical parameters to the controlled particle size and morphology during a precipitation process.[6−9]

The physical and chemical instabilities are the major challenges with the colloidal nanoparticle systems. The high ionic strength and variation in pH of the environment make the design of drugs and drug carrier systems to be delivered to the human body especially difficult. Typically surfactants and/or polymers are used to stabilize nanosuspensions by preventing aggregation and agglomeration. These also have been shown to have a pronounced effect on the *in vivo* behavior.[10] Most of the commonly used materials suffer from the fact that the particles are not stable indefinitely and aggregation might occur during storage or when the suspension is dried. To overcome stability problems as well as poor bioavailability or biocompatibility challenges, new strategies including new materials must be explored.

*Address correspondence to hanna.valo@helsinki.fi.

Received for review December 3, 2009 and accepted February 23, 2010.

Published online March 8, 2010.
10.1021/nn9017558

On the other hand, stability of the system is not the only requirement for successful drug delivery *via* nanoparticles. Drug carrier systems without nonspecific interactions with cells and proteins are quickly cleared from the bloodstream or cannot be accumulated in targeted tissue.[11,12] To achieve active targeting, specific ligands have to be attached to the surface of the drug carrier. In addition to permeation, absorption, and targeting aspects, the surface properties of the carrier system have a major influence also on the formulation stability.[13]

Hydrophobins form a family of amphiphilic proteins having the ability to form self-assembled monolayers on hydrophobic materials.[14] This results in lower surface free energy and formation of a protein shell around hydrophobic particles, which both facilitates the dispersion in water and protects the particles against aggregation. The protein coating can then be modified in various ways to gain other benefits such as assembly on a target surface or controlled release rate. The protein used in the present study was a class II hydrophobin (HFBII) expressed in *Trichoderma reesei*.[15] Hydrophobins have been divided into two classes on the basis of the hydropathy nature of their amino acid sequences. These classes also have significant differences among the solubility of the assembled structures they form.[16] The class II hydrophobins (*e.g.*, HFBI, II, and III) are small, less than 10 kD, and they can be easily dissolved at rather high concentrations in aqueous solutions.[17−19] Class I (*e.g.*, SC3) hydrophobins form highly insoluble structures, which can be disassembled only by treatment with strong acids.[20] Hydrophobins are not toxic by themselves[21] and have actually been shown to prevent immune responses by forming a surface layer on the airborne fungal spores,[22] making them a highly attractive material for applications for release of drugs or food ingredients.

Because of the amphiphilic nature of hydrophobins, their adsorption to hydrophobic/hydrophilic interfaces without losing their folded structure is possible.[17] Their ability to self-assemble onto various structures and to form stable films at interfaces is essential for fungal growth in biology. But this feature is also extremely fascinating when considering engineered nanotechnological approaches.[17,23−25] Existing applications of hydrophobins utilize the adsorption of class I hydrophobins to increase the bioavailability of poorly soluble drugs,[26] modify surfaces,[27−30] predict extreme foaming tendency,[31] and stabilize bubbles and foams.[32] In pharmaceutical research, utilizing the hydrophobin fusion proteins with variable chemical groups can offer options in the area of controlled and targeted drug delivery.

Inspired by the stability, adsorption properties, and versatile character of hydrophobins,[14,33] experiments to produce hydrophobin-coated drug nanoparticles were performed. The proof of concept study was done using a low-solubility model drug compound, beclomethasone dipropionate (BDP). Adsorption of the amphiphilic stabilizer onto the particle surface from an aqueous solution was used to stabilize the BDP nanoparticles and prevent their growth. Additionally, specific functional sites on the particle surface could be realized by utilizing modified HFB proteins bound to another protein. In this study, the combination of protein bioengineering and traditional pharmaceutical technology was used to synthesize functionalized protein-coated nanoparticles for drug delivery purposes.

RESULTS AND DISCUSSION

Adsorption of the Multifunctional Protein on the Nanoparticles. Earlier studies have shown that the process parameters have major effects on particle size, morphology, and recovery rate when antisolvent precipitation of BDP or other poorly water-soluble drugs is carried out with and without[6] surface active agents.[34,35] Pharmaceutical excipients such as surfactants are commonly added during the crystallization processes to control the particle growth and the surface properties.[36,37] By increasing the amount of the surfactant, mean particle size in colloid dispersions can be reduced.[38] Particles also maintain their size better after freeze-drying with higher surfactant amounts.[39] In our studies, experiments showed that particle size and morphology were affected strongly by increasing the concentration of the surface active protein HFBII. Examples of TEM images from the particles precipitated with varying amounts of HFBII are shown in Figure 1. The amount of BDP was kept constant (0.05% (w/v)) in each experiment. At low contents of HFBII, 0−0.005% (w/v), BDP precipitation yielded rods that were several micrometers long (Figure 1a,b). When HFBII concentration was gradually increased above 0.008% (w/v), particle

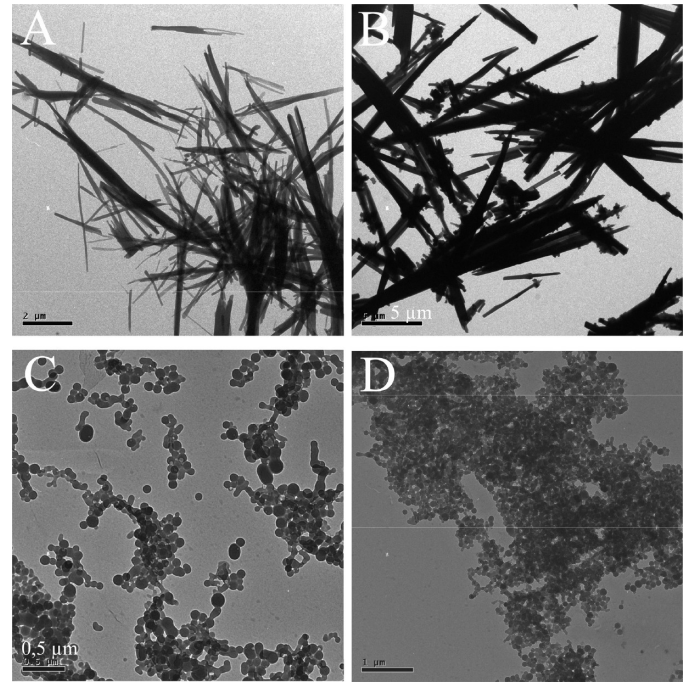

Figure 1. TEM images showing BDP precipitation in deionized water (A) without HFBII, (B) with 0.005% HFBII, (C) with 0.05% HFBII, (D) with 0.1% HFBII.

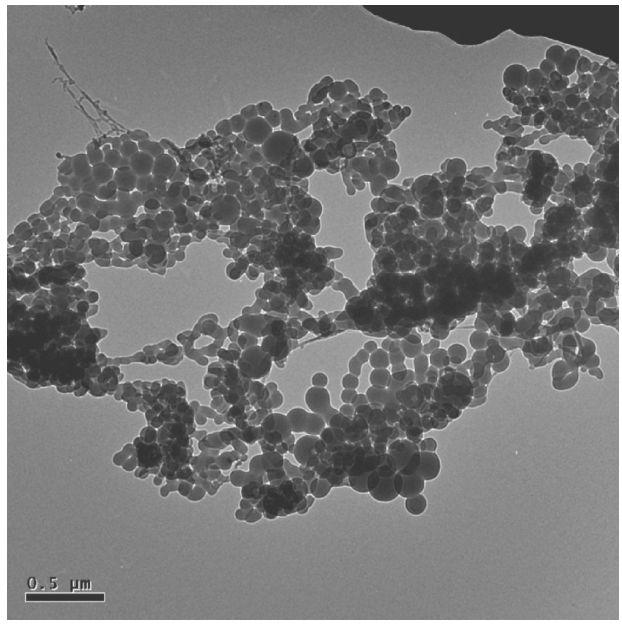

Figure 2. TEM images showing freeze-dried HFBII-coated BDP particles.

size was decreased below 200 nm and the rodlike crystals were transformed into spherical ones (Figure 1c,d). On the basis of the TEM results, 0.05% HFBII concentration was selected for further studies. At this point, particle size was 103 ± 27 nm, and a narrow particle size distribution (D10/D50/D90; 72/101/134 nm) was obtained. The morphological change of the resulting particles seemed to be quite abrupt with no clear transition state, and no more changes in the particle size or shape were observed with HFBII concentrations exceeding the threshold (see Supporting Information). Presumably, adsorption of the amphiphilic stabilizer (HFBII) onto the particle/water interface limited the crystal growth of BDP.[36] About 50% of HFBIIs hydrophobic side chains are on the surface on one side of the protein.[14] This makes a part of the protein surface hydrophobic and enables physical adsorption which is based on interactions between hydrophobic areas of protein and drug. Hydrophobin adsorption is known to be strong at solid−liquid interfaces depending on the hydrophobicity of the surface area.[25,27] Thus, HFBII can be effectively used to provide stabilization for hydrophobic drugs and in the production of drug nanoparticles.

The physical stability of the particles in suspension was examined at room temperature and in an ice bath under low stirring rate. In ambient conditions, room temperature, and pH 5, the particles in the suspension started to show shape changes already after 1.5 h. This could be increased to at least 5 h when the pH was adjusted to 8 and the sample was stored in an ice-bath under mild stirring. After that, irreversible aggregates and crystal shape changes were observed by TEM in spite of the cold storage temperature (see Supporting Information). Thus, it can be concluded that HFBII restricts particle growth efficiently, but does not prevent aggregation indefinitely. The isoelectric point (pI) of HFBII has been determined to be at pH 4.8.[40] At the pI, the charge of the protein is near zero and electrostatic stabilization of the particles is negligible. Because the steric stabilization was not adequate alone, a tendency toward aggregation is obvious unless the pH is adjusted. This was shown by the more than 2.5 fold increase in the stability of the suspension at pH 8, where HFBII has a negative charge.

Since BDP−HFBII nanoparticles showed poor long-term stability in suspension, freeze-drying was introduced. The stability of nanoparticles in the dry state has been improved notably by freeze-drying processes,[41] where the suspension is rapidly frozen and the solvent sublimated at controlled pressure and temperature. Freeze-drying was shown to be an efficient way to improve stability of BDP−HFBII nanoparticles, which were aggregated irreversibly when dried at room temperature and at normal air pressure. A TEM image of freeze-dried nanoparticles taken after 3 days of storage is presented in Figure 2.

As was shown already, the physicochemical characteristics of the adsorped excipients have an impact on the particle growth and stability during and after the precipitation and drying processes. This also determines, to a large degree, the potential of the formulation for further development. As the characteristics of the HFB-coated nanoparticles seemed promising, they were studied in more detail.

Characterization of the Coated Nanoparticles. Accurate characterization and knowledge of the formulation and the physical state of the drug is of fundamental interest because it affects the solubility, drug release rate, permeability, and degradation in the body. Variable temperature X-ray powder diffractometry (VT-XRPD) and differential scanning calorimetry (DSC) were used to investigate the effect of the precipitation process and formation of the protein coating on the crystallinity of the drug and to gain more information on possible interactions between the drug and the protein. Changes in glass transition (T_g) or melting (T_m) temperatures or changes in the XRPD patterns would indicate possible interactions between the drug and the protein matrix or polymorphic changes. The larger volume-to-surface areas of the nanoparticles[42] and their shape[43] were also expected to have an effect on the thermal behavior. In the XRPD, changes in crystal structures were observed by heating the samples gradually to set temperatures based on the DSC thermograms.

The DSC thermogram of precipitated pure BDP exhibited an endothermic peak at around 80 °C indicating a structural change where the water was removed from the crystal lattice (Figure 3). The VT-XRPD pattern confirmed (Figure 4A) the transformation of monohydrate to anhydrate form at 55−90 °C. At 210 °C, the drug melted at the same temperature as the original powder (data not shown). The pure HFBII (Figure 3) showed a small and

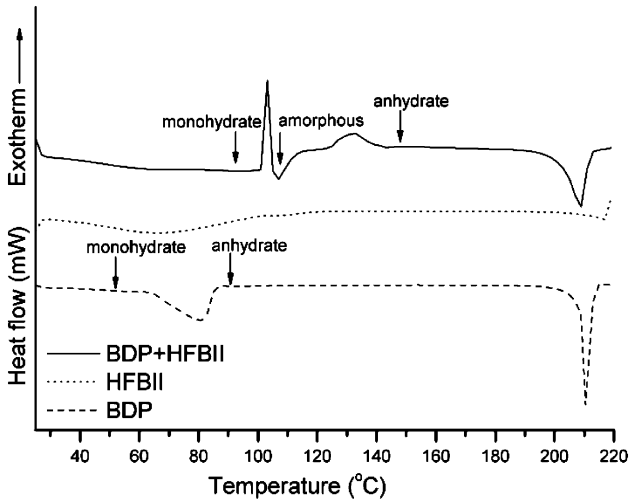

Figure 3. DSC thermograms of precipitated BDP (dashed line), HFBII (dotted line), and BDP (solid line) precipitated with 0.05% HFBII. Arrows indicate the crystal structures based on the VT-XRPD results.

broad endothermic change at 40−120 °C. On the basis of the XRPD results it was completely amorphous.

With the BDP−HFBII nanoparticles, exothermic peaks, which were not present in the thermogram of pure precipitated BDP (Figure 3), were observed at around 102 and at 132 °C. It has been reported that amorphous BDP has a T_g at around 100 °C, and its crystallization temperature is at *ca.* 130−140 °C to anhydrate form.[44] However, on the basis of the XRPD results, the BDP was at least partly in monohydrate form until the temperature crossed 90 °C (Figure 4B). Above that, amorphous material dominated until at 145 °C the amorphous BDP crystallized into its anhydrate form. On the basis of these results, BDP coated with HFBII are likely to form an amorphous mixture during the warming cycle in DSC/XRPD. The viscous amorphous form would then be the reason for the retarded crystalline change of BDP. Because of the small particle size of the nanoparticles, the absence of any distinct diffraction peaks and weaker intensities in their XPRD patterns does not necessarily indicate a decrease or lack of crystallinity in the samples. The melting of the anhydrate BDP−HFBII occurred at 210 °C, which is also the melting temperature of the reference samples. The heat of melting of the nanoparticles was equal to the precipitated BDP, although the peak was slightly broader probably due to differences in the crystal size.

Saturated solubilities of BDP−HFBII nanoparticles and the precipitated BDP microparticles to 35% ethanol were 35.6 and 27.8 μg/mL, respectively (Figure 5). Complete solubility was reached within 60 min in both cases and the extent was increased by *ca.* 30% for the BDP−HFBII nanoparticle formulation. The saturation solubilities of bulk BDP and physical mixture of BDP−HFBII were also studied. The solubility of BDP with HFBII increased 30% as well compared with BDP without HFBII. Thus, improvement of solubility in nanoparticle formulation was mainly due to the free HFBII and is similar to the solubility increase with simple surfactants such as Tween-80.[45] The solubility of nanoparticles should increase with decreasing size,[46] but this was not observed here. During the solubility test, HFBII bound to the surfaces of BDP particles did not restrict the dissolution. On the other hand, desorption of HFBII might have caused aggregation of BDP, and therefore improvement of the solubility was not higher.

On the basis of the DSC and VT-XRPD, we conclude that after the precipitation processes BDP was in its

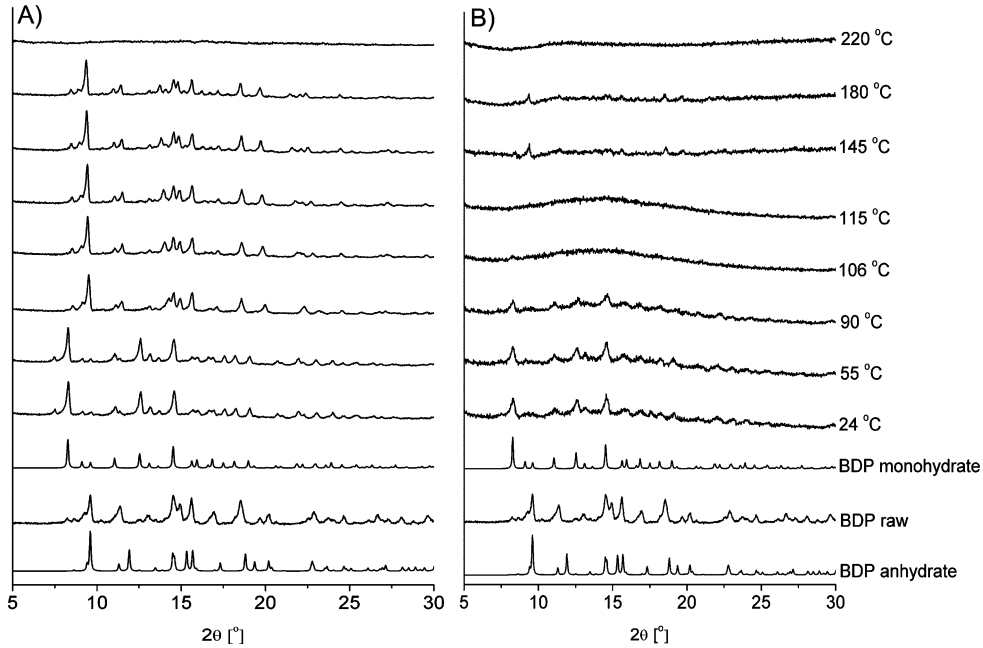

Figure 4. (A) VT-XRPD of precipitated BDP without HFBII at various temperatures; (B) VT-XRPD of precipitated BDP nanoparticles with HFBII at various temperatures. Reference patterns are shown at the bottom of the figures.

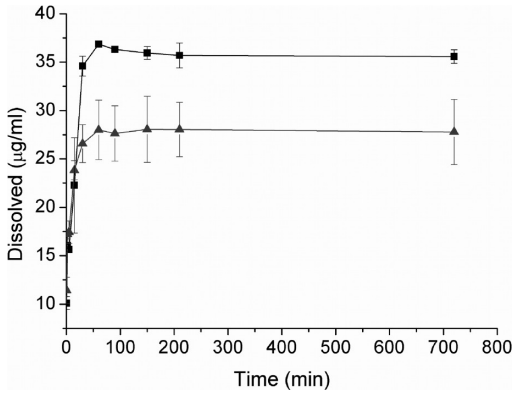

Figure 5. Saturation solubility profiles of BDP−HFBII (1:1 weight ratio) nanoparticle suspension (top) and BDP microparticle suspension (bottom). In nanosuspensions the particle size was 103 ± 27 nm, and in BDP the microparticle suspensions were several micrometers (n = 2).

monohydrate form. The presence of an HFBII coating did have an effect on the removal of the water from the crystal structure. This was due to HFBII and BDP forming an amorphous mixture before BDP crystallized into its anhydrate form. The prepared nanoparticles showed slightly higher solubility values compared to the precipitated BDP microparticles.

Functionalization of the BDP−HFB Nanoparticles. As the BDP−HFB nanoparticles were shown to be relatively stable and the solubility of BDP was improved, the next step was to study their functionalization. This was done by two approaches: embedding an additional compound onto the HFB surface by electrostatic forces and by using fusion proteins, where a functional group was introduced by covalently bonding it to the protein shell. In the first test, BDP−HFBII nanoparticles were decorated with 3 nm mercaptosuccinic acid (MSA)-coated Au nanoparticles.

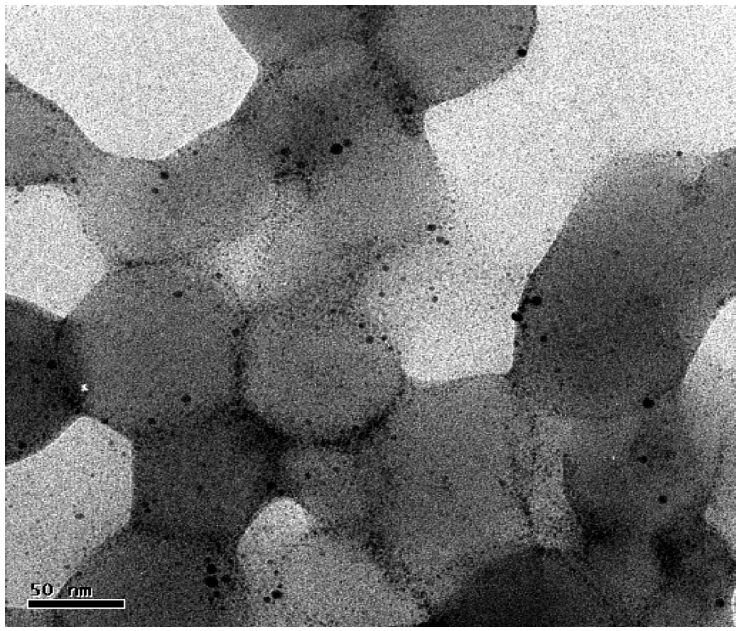

Figure 6. BDP−HFBII nanoparticles decorated with 3 nm mercaptosuccinic acid (MSA)-coated Au nanoparticles.

The Au nanoparticles could be seen to strongly adsorb at the interfaces of BDP−HFBII nanoparticles, which could be seen as improved contrast for microscopical imaging as shown in Figure 6. Labeling could be useful for localization of the drug nanoparticles in electron microscopy or as an alternative route for functionalizing the surface. Several routes for producing Au nanoparticles with functional organic shells have been proposed.[47−49] As the Au nanoparticles are bound to the drug particles *via* electrostatic interactions, surface association was also observed to some extent in the BDP microparticles having no protein coating (see Supporting Information).

Another type of labeling of the BDP nanoparticles was done by utilizing a green fluorescent protein−hydrophobin fusion protein GFP−HFBI. The fusion protein was incorporated into the particle surface either during the precipitation step or after synthesis, as was done in the case of the BDP microparticles. HFBI and HFBII have very similar sizes and behavior and, thus, GFP−HFBI and HFBII are expected to form mixed monolayers on particle surfaces. As a simple test of the interfacial properties of the GFP−HFBI, its adhesion onto water−air interface was first studied. As can be seen from Figure 7, the protein strongly concentrates at the interface between water and air. It also forms some needle-like structures in water,[24] which are shown as bright green patterns in the fluorescence microscopy image (Figure 7). This is a well documented feature of HFBII, and the strong fluorescence shows that the GFP−HFBI fusion coassembles well with the wild-type hydrophobin.

GFP−HFBI gravitated toward air−water (as shown in the Figure 7) and solid-water interfaces (as show in the Figure 8), and thus the GFP−HFBI label could be seen to strongly adsorb onto the BDP microparticles (Figure 8). The particles were much easier to find using the fluorescence detector than using white light illumination with 100× magnification. Although the air bubbles in the solution were also stained by the GFP, the particle agglomerates could be easily found and identified with the microscope. We studied and identified, with the TEM, that the precipitation process of BDP with HFBII and GFP−HFBI produced nanosized drug particles. In the case of the nanoparticles (Figure 9), it was almost impossible to find the particles using just the white light mode, as focusing on the small particles was next to impossible. The fluorescence marker, however, could be clearly seen, and the particle masses could be detected in that mode. Thus, the labeling was successful and clearly demonstrates the surface functionalization of the BDP nanoparticles.

CONCLUSIONS

By utilizing multifunctional surface-active proteins and a simple antisolvent−solvent precipitation method, small (<200 nm) protein-

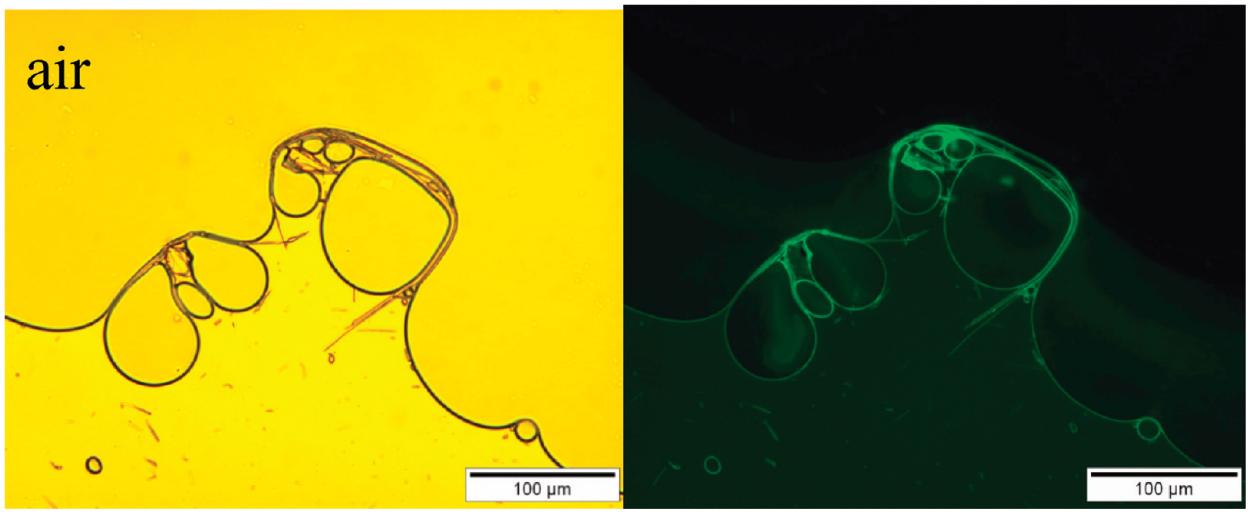

Figure 7. Bright field (left) and fluorescence (right) microscope images of GFP−HFBI assembled at an air−water interface. Free GFP−HFBI in water stains the water phase light green. The water−air interface has a higher concentration of the surface active protein and is therefore brighter green. The protein can also been seen to form needle-like structures in water.

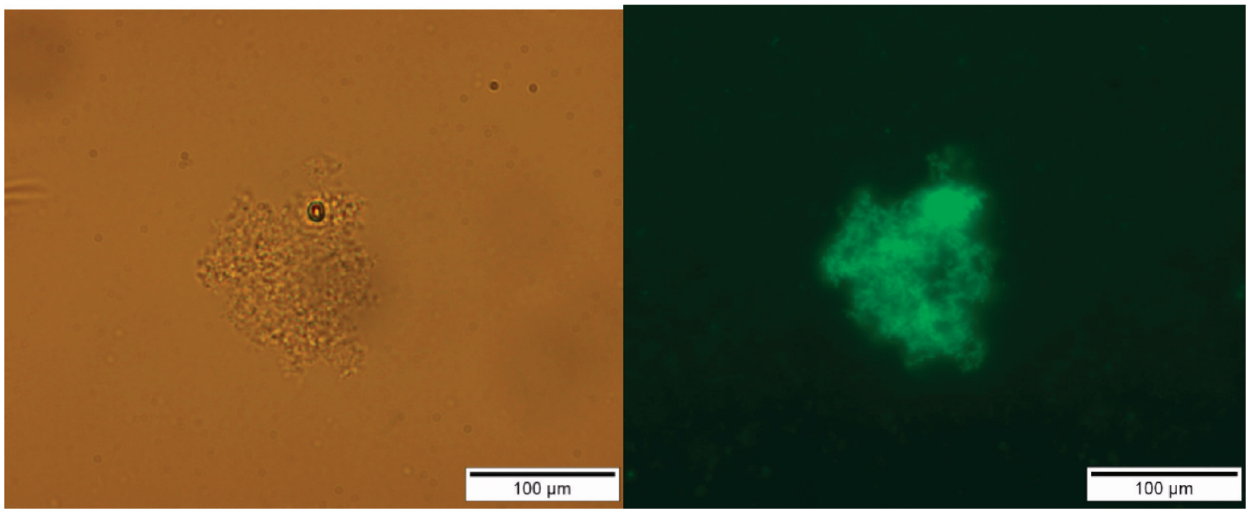

Figure 8. Light (left) and fluorescence (right) microscope images of GFP−HFBI/HFBII (1:3)-coated BDP microparticles. Particles were first precipitated in pure water, and the protein coating was added afterward. Free GFP−HFBI in water stains the water phase light green. The water−BDP interface has a higher concentration of the protein and is therefore brighter green.

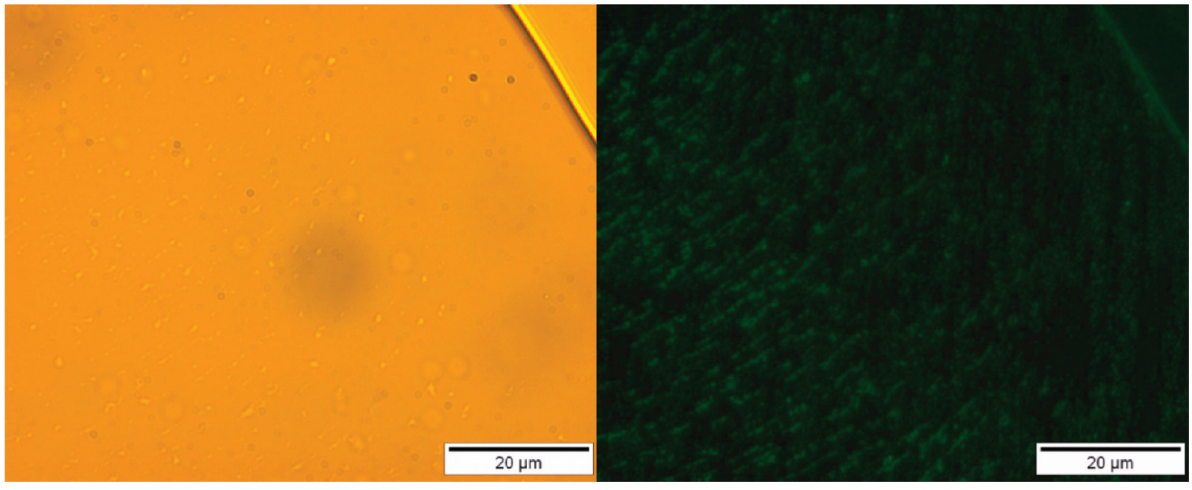

Figure 9. Light (left) and fluorescence (right) microscope images of GFP−HFBI/HFBII (1:3)-coated BDP nanoparticles. The nanoparticles were too small to properly focus on with the conventional light microscope but can be seen in the fluorescence image. Free GFP−HFBI in water stains the water phase light green. The water−BDP interface has a higher concentration of the protein and is therefore brighter green.

coated drug particles were produced. Adsorption of the amphiphilic class II hydrophobins onto the particle−liquid interfaces during the precipitation process gave three notable effects: (i) it arrested particle growth, (ii) it offered a way to improve stability, and (iii) it provided a layer around the hydrophobic drug that is possible to functionalize. Labeling studies clearly demonstrated that the surface of the nanoparticles was covered with the hydrophobins. A tailored group on the hydrophilic side of the protein can be designed for specific functions by using protein engineering tools. The group could, for example, be the binding domain for an advanced delivery system, or it could also be a targeting group to enhance cell wall penetration or localization of the drug. Thus, bioavailability could be increased not only by the increased solubility *via* small size of the drug particles, but the increased permeation as well. We propose that the presented system could act as a basis for advanced multifunctional drug nanoparticles, where improved bioavailability and targeting could be combined in a one well-defined system.

METHODS

Materials. The model drug was beclomethasone dipropionate (Sigma, St. Louis, MO). HFBII[15] and GFP−HFBI[50] were expressed and purified as described elsewhere. In the GFP−HFBI fusion protein GFP was genetically fused to HFBI by a short peptide linker. Methanol (Riedel-de Haën, Seelze, Germany) was used as a solvent in the precipitation process, and ethanol (96%, v/v) (Primalco, Rajamäki, Finland) was used in the dissolution media. The water used was ultrapurified (Millipore, Molsheim, France). All other chemicals were of analytical grade obtained from standard sources and used without further purification.

Precipitation Process. A 34.8 mM beclomethasone dipropionate (BDP, MW = 521.1) solution was prepared by dissolving BDP in methanol. A 0.5 mL portion of BDP solution was poured into 20 mL of 0.05% HFBII in pure deionized water. In all further studies the drug−protein ratio was 1:1. Variable amounts of HFBII, 0−0.15 wt % (0−208.3 μM), were used to determine the effect of the HFBII concentration on crystal habit and size of drug particles. Solutions were filtered with 0.45 μm and BDP solutions with 0.2 μm (Whatman, Brentford, UK) syringe filters to remove possible impurities prior to use. The receiving liquid was stirred vigorously with a magnetic stirrer, and the temperature of the solution was controlled by keeping the sample in an ice bath. The precipitate was observed as a turbid solution immediately after BDP addition. For further analysis, suspensions were dried in a freeze-dryer.

Freeze-Drying of Nanoparticles. For further analysis, the suspensions were frozen by pipetting them dropwise into liquid nitrogen (−196 °C) and immediately placed into a freeze-drying chamber (Kinetics Thermal Systems Lyostar II). Particle dispersions were dried on the freeze-dryer without cryo- or lyoprotectants. The primary drying was performed at −30 °C for 72 h followed by the secondary drying, where the temperature was first increased to −10 °C for 4 h, then to −5 °C for 18 h, and then to 0 °C for 2 h. Pressure was maintained at 150 mTor (20 Pa). Powders were analyzed immediately after drying by XRPD and DSC. TEM-images from the dry powder were taken after 3 days of storage in the vacuum dessicator.

Differential Scanning Calorimetry Experiments. Thermal behavior of the nanopowders was determined using a differential scanning calorimeter (Mettler Toledo, Columbus, OH). The samples were held at 25 °C for 5 min before heating. All the samples were heated from 25 to 250 °C and cooled down to 25 °C. The heating rate was 10 °C min^{-1}, and cooling rate was 20 °C min^{-1}. The data was analyzed with STARe software (Mettler Toledo, Columbus, OH).

VT-XRPD Experiments. VT-XRPD patterns were determined from the pure materials, precipitated BDP, and the BDP−HFBII nanoparticle formulations. The VT-XRPD was performed using the θ−θ diffractometer (Bruker AXS D8, Karlsruhe Germany). The experiments were performed in symmetrical reflection mode with Cu Kα radiation (1.54 Å) using Göbel Mirror bent gradient multilayer optics. The scattered intensities were measured with a scintillation counter. The angular range was from 5° to 40°. The measurements were made with the steps of 0.02°, and the measuring time was 2 s/step. Samples were heated to 24, 55, 90, 106, 115, 145, 180, and 220 °C at a speed of 10 °C/min and kept at the assigned temperatures during each measurement. The reference data (anhydrate and monohydrate forms of BDP) were retrieved from the Cambridge Structural Database (CSD) using the ConQuest program.

Morphology and Size. Characterization of the particle size and morphology was done by transmission electron microscope (FEI Tecnai F12, Philips Electron Optics, The Netherlands). Nanoparticle dispersions were dried or spread (freeze-dried powder) on Formvar film-coated copper grids with a mesh size of 300 (Agar Scientific, Essex, U.K.).

Labeling BDP Nanoparticles with a Fluorescent Marker. Synthesis of GFP−HFBI-labeled nanoparticles was carried out in the same manner as with the normal nanoparticles, except that a part of the HFBII was partly replaced with the GFP−HFBI fusion protein.[50] The two proteins were dissolved in 1:3 ratio (GFP−HFBI/HFBII) in pure deionized water prior to the synthesis. All other steps remained the same. The GFP labeling of microparticles was done after the synthesis by adding GFP−HFBI to the solution containing BDP particles. Synthesis itself was simple precipitation of BDP from methanol into water.

Labeling BDP Nanoparticles with the Au-Nanoparticles. Mercaptosuccinic acid (MSA)-coated Au-nanoparticles were produced by the Kimura method.[51] Labeling by MSA−Au nanoparticles was carried out after the production of the BDP−HFBII nanoparticles by simply adding 10 μL of 0.35 mg/mL MSA−Au particle solution to 20 μL of the BDP−HFBII particle suspension. The suspension was allowed to stand for 1 h before taking samples for the TEM.

Fluorescence Microscope Studies of the Particles. A small drop of GFP−HFBI/HFBII-coated BDP nanoparticle suspension was pipetted on microscope slides directly from the synthesis solution. Both bright field and fluorescent imaging was done by Olympus BX-50 microscope. Emission light was filtered with a WG Filter (510−550 nm) in fluorescence imaging of GFP−HFBI.

Saturated Solubility. Dissolution behavior of the precipitated particles was studied using 40 mL of 36% (v/v) ethanol as dissolution medium, with magnetic stirring at a speed of 100 rpm. The solubility of BDP is so low that the use of ethanol as dissolution medium is reasoned for detection aspects. The temperature was maintained at 37 ± 0.5 °C (Sotax AT7, Perkin-Elmer Lambda 2). A 4 ml (0.5 mg/mL) portion of cold nanoparticle suspension was added to dissolution media in 15 s. Samples (0.6 mL) were taken at various time points, and the extracted medium was replaced. The samples were centrifuged at 13 000 rpm for 10 min and filtered with 0.2 μm (GHD Acrodisc, PALL Life Sciences, USA) syringe filters. The released amount of BDP was determined by a UV spectrophotometer (Agilent 1100 series) at a wavelength of 242 nm.

Acknowledgment. Riitta Suihkonen is thanked for technical assistance and Jussi Joensuu for kindly providing the GFP−HFBI. Petteri Heljo is acknowledged for his expert help with the freeze-dryer. We gratefully acknowledge the financial support from the University of Helsinki (Development of Nano Sciences/HENAKOTO, 700036). M.B.L. acknowledges the support of the Academy of Finland (Grant No. 118519).

Supporting Information Available: Additional TEM images. This material is available free of charge *via* the Internet at http://pubs.acs.org.

REFERENCES AND NOTES

1. Hillaireau, H.; Couvreur, P. Nanocarriers' Entry into the Cell: Relevance to Drug Delivery. *Cell. Mol. Life. Sci.* **2009**, *66*, 2873–2896.
2. Peltonen, L.; Hirvonen, J. Physicochemical Characterization of Nano- and Microparticles. *Curr. Nanosci.* **2008**, *4*, 101–107.
3. Marcucci, F.; Lefoulon, F. Active Targeting with Particulate Drug Carriers in Tumor Therapy: Fundamentals and Recent Progress. *Drug Discovery Today* **2004**, *9*, 219–228.
4. Müller, R. H.; Peters, K. Nanosuspensions for the Formulation of Poorly Soluble Drugs: I. Preparation by a Size-Reduction Technique. *Int. J. Pharm.* **1998**, *160*, 229–237.
5. Bilati, U.; Allémann, E.; Doelker, E. Development of a Nanoprecipitation Method Intended for the Entrapment of Hydrophilic Drugs into Nanoparticles. *Eur. J. Pharm. Sci.* **2005**, *24*, 67–75.
6. Wang, Z.; Chen, J.; Le, Y.; Shen, Z.; Yun, J. Preparation of Ultrafine Beclomethasone Dipropionate Drug Powder by Antisolvent Precipitation. *Ind. Eng. Chem. Res.* **2007**, *46*, 4839–4845.
7. Keck, C. M.; Müller, R. H. Drug Nanocrystals of Poorly Soluble Drugs Produced by High Pressure Homogenisation. *Eur. J. Pharm. Biopharm.* **2006**, *26*, 3–16.
8. Matteucci, M. E.; Hotze, M. A.; Johnston, K. P.; Williams, R. O. Drug Nanoparticles by Antisolvent Precipitation: Mixing Energy *versus* Surfactant Stabilization. *Langmuir* **2006**, *22*, 8951–8959.
9. Galindo-Rodriguez, S.; Allémann, E.; Fessi, H.; Doelker, E. Physicochemical Parameters Associated with Nanoparticle Formation in the Salting-out, Emulsification−Diffusion, and Nanoprecipitation Methods. *Pharm. Res.* **2004**, *21*, 1428–1439.
10. Patravale, V. B.; Date, A. A.; Kulkarni, M. R. Nanosuspensions: A Promising Drug Delivery Strategy. *J. Pharm. Pharmacol.* **2004**, *56*, 827–840.
11. Torchilin, V. P. Polymer-Coated Long-Circulating Microparticulate Pharmaceuticals. *J. Microencapsulation* **1998**, *15*, 1–19.
12. Bae, Y. H. Drug Targeting and Tumor Heterogeneity. *J. Controlled Release* **2009**, *133*, 2–3.
13. Couvreur, P.; Gref, R.; Andrieux, K.; Malvy, C. Nanotechnologies for Drug Delivery: Application to Cancer and Autoimmune Diseases. *Prog. Solid State Chem.* **2006**, *34*, 231–235.
14. Linder, M. B. Hydrophobins: Proteins That Self Assemble at Interfaces. *Curr. Opin. Colloid Interface Sci.* **2009**, *14*, 356–363.
15. Linder, M.; Selber, K.; Nakari-Setala, T.; Qiao, M.; Kula, M.; Penttila, M. The Hydrophobins HFBI and HFBII from *Trichoderma reesei* Showing Efficient Interactions with Nonionic Surfactants in Aqueous Two-Phase Systems. *Biomacromolecules* **2001**, *2*, 511–517.
16. Wessels, J. G. H. Developmental Regulation of Fungal Cell Wall Formation. *Annu. Rev. Phytopathol.* **1994**, *32*, 413–437.
17. Linder, M. B.; Szilvay, G. R.; Nakari-Setälä, T.; Penttilä, M. E. Hydrophobins: The Protein-Amphiphiles of Filamentous Fungi. *FEMS Microbiol. Rev.* **2005**, *29*, 877–896.
18. Wösten, H. A. B. Hydrophobins: Multipurpose Proteins. *Annu. Rev. Microbiol.* **2001**, *55*, 625–646.
19. Nakari-Setälä, T.; Aro, N.; Ilmén, M.; Muñoz, G.; Kalkkinen, N.; Penttilä, M. Differential Expression of the Vegetative and Spore-Bound Hydrophobins of *Trichoderma reesei*. *Eur. J. Biochem.* **1997**, *248*, 415–423.
20. de Vocht, M. L.; Scholtmeijer, K.; van der Vegte, E. W.; de Vries, O. M. H.; Sonveaux, N.; Wösten, H. A. B.; Ruysschaert, J.; Hadziioannou, G.; Wessels, J. G. H.; Robillard, G. T. Structural Characterization of the Hydrophobin SC3, as a Monomer and after Self-Assembly at Hydrophobic/Hydrophilic Interfaces. *Biophys. J.* **1998**, *74*, 2059–2068.
21. Ebbole, D. J. Hydrophobins and Fungal Infection of Plants and Animals. *Trends Microbiol.* **1997**, *5*, 405–408.
22. Aimanianda, V.; Bayry, J.; Bozza, S.; Kniemeyer, O.; Perruccio, K.; Elluru, S. R.; Clavaud, C.; Paris, S.; Brakhage, A. A.; Kaveri, S. V.; *et al*. Surface Hydrophobin Prevents Immune Recognition of Airborne Fungal Spores. *Nature* **2009**, *460*, 1117–1121.
23. Linder, M.; Szilvay, G. R.; Nakari-Setälä, T.; Söderlund, H.; Penttilä, M. Surface Adhesion of Fusion Proteins Containing the Hydrophobins HFBI and HFBII from *Trichoderma reesei*. *Protein Sci.* **2002**, *11*, 2257–2266.
24. Torkkeli, M.; Serimaa, R.; Ikkala, O.; Linder, M. Aggregation and Self-Assembly of Hydrophobins from *Trichoderma reesei*: Low-Resolution Structural Models. *Biophys. J.* **2002**, *83*, 2240–2247.
25. Laaksonen, P.; Kivioja, J.; Paananen, A.; Kainlauri, M.; Kontturi, K.; Ahopelto, J.; Linder, M. B. Selective Nanopatterning Using Citrate-Stabilized Au Nanoparticles and Cystein-Modified Amphiphilic Protein. *Langmuir* **2009**, *25*, 5185–5192.
26. Haas Jimoh Akanbi, M.; Post, E.; Meter-Arkema, A.; Rink, R.; Robillard, G. T.; Wang, X.; Wösten, H. A. B.; Scholtmeijer, K. Use of Hydrophobins in Formulation of Water Insoluble Drugs for Oral Administration. *Colloids Surf., B* **2009**, *75*, 526–531.
27. Lumsdon, S. O.; Green, J.; Stieglitz, B. Adsorption of Hydrophobin Proteins at Hydrophobic and Hydrophilic Interfaces. *Colloid Surf., B* **2005**, *44*, 172–178.
28. Janssen, M. I.; van Leeuwen, M. B. M.; Scholtmeijer, K.; van Kooten, T. G.; Dijkhuizen, L.; Wösten, H. A. B. Coating with Genetic Engineered Hydrophobin Promotes Growth of Fibroblasts on a Hydrophobic Solid. *Biomaterials* **2002**, *23*, 4847–4854.
29. Scholtmeijer, K.; Janssen, M. I.; Gerssen, B.; de Vocht, M. L.; van Leeuwen, B. M.; van Kooten, T. G.; Woesten, H. A. B.; Wessels, J. G. H. Surface Modifications Created by Using Engineered Hydrophobins. *Appl. Environ. Microbiol.* **2002**, *68*, 1367–1373.
30. De Stefano, L.; Rea, I.; Armenante, A.; Giardina, P.; Giocondo, M.; Rendina, I. Self-Assembled Biofilm of Hydrophobins Protects the Silicon Surface in the KOH Wet Etch Process. *Langmuir* **2007**, *23*, 7920–7922.
31. Sarlin, T.; Nakari-Setala, T.; Linder, M.; Penttila, M.; Haikara, A. Fungal Hydrophobins as Predictors of the Gushing Activity of Malt. *J. Inst. Brew.* **2005**, *111*, 105–111.
32. Cox, A. R.; Aldred, D. L.; Russell, A. B. Exceptional Stability of Food Foams Using Class II Hydrophobin HFBII. *Food Hydrocolloids* **2009**, *23*, 366–376.
33. Hektor, H.; Scholtmeijer, K. Hydrophobins: Proteins with Potential. *Curr. Opin. Biotechnol.* **2005**, *16*, 434–439.
34. Rogers, T. L.; Gillespie, I. B.; Hitt, J. E.; Fransen, K. L.; Crowl, C. A.; Tucker, C. J.; Kupperblatt, G. B.; Becker, J. N.; Wilson, D. L.; Todd, C.; *et al*. Development and Characterization of a Scalable Controlled Precipitation Process to Enhance the Dissolution of Poorly Water-Soluble Drugs. *Pharm. Res.* **2004**, *21*, 2048–2057.
35. Rasenack, N.; Steckel, H.; Müller, B. W. Micronization of Anti-Inflammatory Drugs for Pulmonary Delivery by a Controlled Crystallization Process. *J. Pharm. Sci.* **2003**, *92*, 35–44.
36. Zimmermann, A.; Millqvist-Fureby, A.; Elema, M. R.; Hansen, T.; Müllertz, A.; Hovgaard, L. Adsorption of Pharmaceutical Excipients onto Microcrystals of Siramesine Hydrochloride: Effects on Physicochemical Properties. *Eur. J. Pharm. Biopharm.* **2009**, *71*, 109–116.
37. Zhang, H.; Wang, J.; Zhang, Z.; Le, Y.; Shen, Z.; Chen, J. Micronization of Atorvastatin Calcium by Antisolvent Precipitation Process. *Int. J. Pharm.* **2009**, *374*, 106–113.
38. Park, K.; Lee, M.; Hwang, K.; Kim, C. Phospholipid-Based Microemulsions of Flurbiprofen by the Spontaneous Emulsification Process. *Int. J. Pharm.* **1999**, *183*, 145–154.
39. Lim, S.; Kim, C. Formulation Parameters Determining the Physicochemical Characteristics of Solid Lipid

Nanoparticles Loaded with All-Trans Retinoic Acid. *Int. J. Pharm.* **2002**, *243*, 135–146.
40. Cox, A. R.; Cagnol, F.; Russell, A. B.; Izzard, M. J. Surface Properties of Class II Hydrophobins from *Trichoderma reesei* and Influence on Bubble Stability. *Langmuir* **2007**, *23*, 7995–8002.
41. Abdelwahed, W.; Degobert, G.; Stainmesse, S.; Fessi, H. Freeze-Drying of Nanoparticles: Formulation, Process and Storage Considerations. *Adv. Drug Delivery Rev.* **2006**, *58*, 1688–1713.
42. Safaei, A.; Attarian Shandiz, M. Size-Dependent Thermal Stability and the Smallest Nanocrystal. *Phys. E* **2009**, *41*, 359–364.
43. Wen, Y.; Fang, H.; Zhu, Z.; Sun, S. Molecular Dynamics Investigation of Shape Effects on Thermal Characteristics of Platinum Nanoparticles. *Phys. Lett. A* **2009**, *373*, 272–276.
44. Eerikäinen, H.; Kauppinen, E. I. Preparation of Polymeric Nanoparticles Containing Corticosteroid by a Novel Aerosol Flow Reactor Method. *Int. J. Pharm.* **2003**, *263*, 69–83.
45. Yiyun, C.; Jiepin, Y. Solubilization of Non-Steroidal Anti-Inflammatory Drugs in the Presence of Tween Series Surfactants. *Phys. Chem. Liq.* **2006**, *44*, 249–256.
46. Nelson, K. G. Kelvin Equation and Solubility of Small Particles. *J. Pharm. Sci.* **1972**, *61*, 479–480.
47. Cao, Y.; Wang, Z.; Jin, X.; Hua, X.; Liu, M.; Zhao, Y. Preparation of Au Nanoparticles-Coated Polystyrene Beads and Its Application in Protein Immobilization. *Colloids Surf., A* **2009**, *334*, 53–58.
48. Ghosh, P.; Han, G.; De, M.; Kim, C. K.; Rotello, V. M. Gold Nanoparticles in Delivery Applications. *Adv. Drug Delivery Rev.* **2008**, *60*, 1307–1315.
49. Lin, Y.; Yu, B.; Lin, W.; Lee, S.; Kuo, C.; Shyue, J. Tailoring the Surface Potential of Gold Nanoparticles with Self-Assembled Monolayers with Mixed Functional Groups. *J. Colloid Interface Sci.* **2009**, *340*, 126–130.
50. Joensuu J. J.; Conley A. J.; Brandly J. E.; Linder M. B; Menassa, R. Hydrophobin Fusions for High-Level Transient Protein Expression and Purification in *Nicotiana benthamiana*. Submitted for publication.
51. Kimura, K.; Takashima, S.; Ohshima, H. Molecular Approach to the Surface Potential Estimate of Thiolate-Modified Gold Nanoparticles. *J. Phys. Chem. B* **2002**, *106*, 7260–7266.